Journal of NUCLEAR SCIENCE and TECHNOLOGY, Supplement 4, p. 350–353 (March 2004)

Transmission and Scattering Experiments Using YAP(Ce) and CsI(Tl)

Sung Ho PARK*, Ji Sung PARK and Jong Kyung KIM
Hanyang University, 17 Haengdang-dong, Seongdong-gu, Seoul 133-791, Korea

In order to develop a new concept of baggage inspection system, an experimental system consisting of a gamma source, detector sets, spectrometry, and counting system is prepared. The X-ray scattered signals from a scanned object can contain the information on the atomic composition of the materials constituting the object while the conventional baggage inspection system uses transmission signals related to mass or electron density. 10 mCi Co-57 is used as a radiation source for scanning the test material in this work. Simple transmission and scattering experiments are performed for various test materials, and the measured results are compared with the calculated values. The experiment results from this work will be used in the verification of reconstruction algorithm which requires transmission and scattering signals at the same time to identify the unknown materials.

KEY WORDS: Inspection System, Compton Scattering, Reconstruction Algorithm

I. Introduction

Since the Sep. 11 act of terror in US, the air traffic security has become much tighter than ever before. The newly created U.S. TSA (Transportation Security Administration) requires to implement screening of all bags even by EDS (Explosive Detection System). Until now, most luggage inspection systems used in airport had been difficult to meet the target specification of EDS as given by ECAC (European Civil Aviation Conference) and FAA (Federal Aviation Administration)[1)]. The specification is as follows:

- A minimum amount of an arbitrary type of explosives has to be detected.
- A high detection safety i.e., probability of detection has been ensured.
- An unequivocal differentiation between hazardous and non-hazardous substances has to be ensured.
- Detection of substances independent of shape, position or orientation.

With the conventional X-ray inspection system, it is possible to detect the shapes or forms of objects inside the baggage, but not possible to get information about the composition of the material inside it[2)]. Dual energy technique[3-5)], coherent technique[6)] and Compton scattering techniques[7,8)] are, therefore, suggested to solve this problem.

Among them, a theoretical study to develop a scattering type baggage inspection system has been conducted through an experimental simulation at Hanyang University[9)]. The measured transmission and scattering signals are used in reconstruction algorithm, developed at Hanyang University, to quantify the material properties[10)]. In this paper, the results of some fundamental experiments for developing an improved inspection system were presented.

* Corresponding author: Tel. +82-2-2299-1732, Fax. +82-2-2294-4800, E-Mail; michael@nural.hanyang.ac.kr

II. Methods and Materials

1. Sources and Detectors

Co-57 is selected as an adequate radiation source emitting photons whose energy is similar to the average energy emitted from X-ray generator. Co-57 has mainly three peaks, 14.41 keV(9.5 %), 122.07 keV(85.6%), and 136.43 keV(10.6%). The activity of the source is 10 mCi and the schematic drawing of the source is shown in **Figure 1**.

The developing reconstruction algorithm requires transmission and scattering signals at the same time to identify the unknown materials[9)]. Two kinds of detectors are used for transmission and scattering experiments. For transmission, since the signal is always so high that the detector needs very short decay time, YAP doped with Ce is selected for the transmission detector. Its decay time is short enough to be 27 ns[11)]. LSO (47 ns) or LuAP (17 ns) is also considerable due to its short decay time[11)]. For scattering, the signal is so weak that the detector needs large detection efficiency, which is proportional to the scintillation efficiency in same measurement conditions. When 1 MeV energy is imparted to the detector, CsI(Tl) could produce 65,000 scintillations, which is more than NaI(Tl) produces. But the emission peak wavelength of 540 nm for CsI(Tl) does not match the absorption peak wavelength of 400 nm for most PMTs. However, when measurements are made using photodiodes with extended response into the red region of the spectrum, the scintillation yield is actually higher than that of any other scintillator. The detectors used in this experiment are shown in **Figure 2**. The left one is 12 mm thick YAP for the transmission detector and the right one is 5 mm thick CsI for the scattering detector.

For the detector collimation, 3 mm thick lead sheets are used to make a box-type collimator.

2. Experimental Setups

For fundamental transmission and scattering experiments, the source, detectors, and test materials are located on the same plane as shown in **Figure 3**.

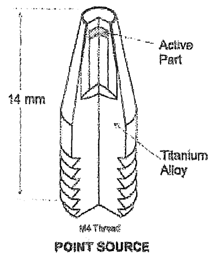

Fig. 1 Schematic Drawing of the Co-57 Point Source

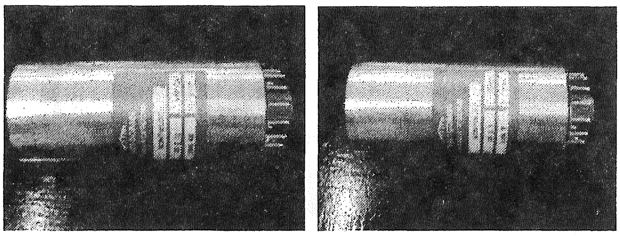

a) b)

Fig. 2 Detectors used in the Experiment: a) YAP for transmission detector, b) CsI for scattering detector

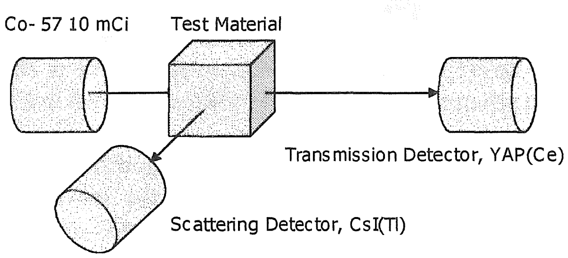

Fig. 3 Schematic Drawing of the Experiment

(1) Source

Co-57 is employed as the experiment source because it has adequate energy to represent the average energy of the 350-450 kVp X-ray generators. For the experiment, source collimator is designed, prepared and checked by using a film. The detailed procedure is stated in the next chapter.

(2) Detectors

Two types of detectors had been considered for the experiment. One was a PMT-supported scintillator, and the other was a photodiode-supported scintillator. Since the former gives better information about the energy spectrum of the scattered photons, it was selected. The thickness of the scintillator was chosen such that it has 100% absorption efficiency for the Co-57 photons. The 12 mm thick YAP and the 5 mm thick CsI have 100% absorption efficiency at 122 keV.

(3) Test Materials

For the experiment, various kinds of test materials were selected. **Table 1** gives the important physical properties of the selected materials. For the convenience of alignment between the source and detectors, each test material was prepared in the form of a cubical block with a 3 cm side.

Table 1. Test Materials and Their Physical Properties

Material	Density g/cm^3	Z_{eff}	Electron density($\times 10^{23}$)
Wood	0.439	6.467	1.08
Polyprophylene	0.897	5.281	3.08
Polyethylene	0.937	5.281	3.22
MC	1.105	6.237	3.59
PVC	1.326	11.998	4.09
Acetal	1.391	6.730	4.46
Aluminum	2.813	13.0	8.16

III. Results and Discussions

1. Source Collimator

The source collimator was designed to meet the general radiation protection regulation such that the dose at the collimator surface should not exceed 1 mR/hr. Lead confined in a steel canister is used as the collimator material. Two kinds of experiments were performed. One is to measure the dose rate and the other is to measure the size of the hole of the collimator by using a film.

Exposure dose rate was measured in front, back, and side part of the collimator as shown in **Figure 4**. The surface dose rate, defined at 10 cm from the surface, in front, back, and side part of the collimator, is 0.45, 0.17, 0.3 mR/hr, respectively.

To measure the size of the collimator hole, a film is contacted with the front part of the collimator for 20 minutes, and then the film is developed and analyzed. The picture of the exposed film and measured dose profiles are shown in **Figure 5**. The dark area in the film is caused by the direct irradiation of Co-57, and thus, the size of the collimator hole can be measured. Analyzing the dose profiles in the graph shown in the upper and right part in **Figure 5**, the diameter of the hole was measured to be 3.74 mm.

2. Transmission and Scattering Spectra

The test block is located at the center of the Co-57 beam. The measured transmission spectrums for various test materials are shown in **Figure 6**. The normalized transmission counts, T, can be expressed by the following equation.

$$T = \exp(-\mu(E)t) \qquad (1)$$

where, μ = total attenuation coefficient of the sample material at 122 keV

t = thickness of the sample, 3 cm

The measured transmission counts and normalized transmission signals calculated from Equation (1) are plotted in **Figure 7** as a function of physical density of the test materials. The transmission counts are decreased as physical density is increased due to the increase of attenuation coefficient. The measured counts are well agreed with the calculated values in most cases. Because the build-up is not considered in the Equation (1), the calculated values are always under-estimated. But, for the PVC, the measured count gives significantly smaller value than the calculated one.

The net counts for the measured transmission spectrum were summarized in **Table 2**.

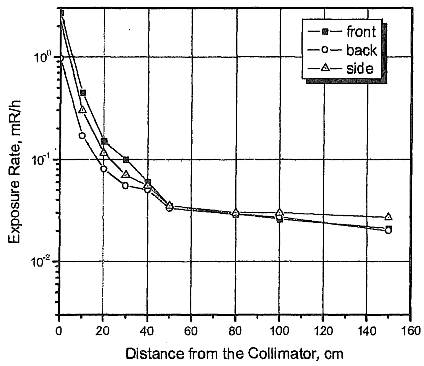

Fig. 4 Exposure Dose Rate Measured by GM Counter

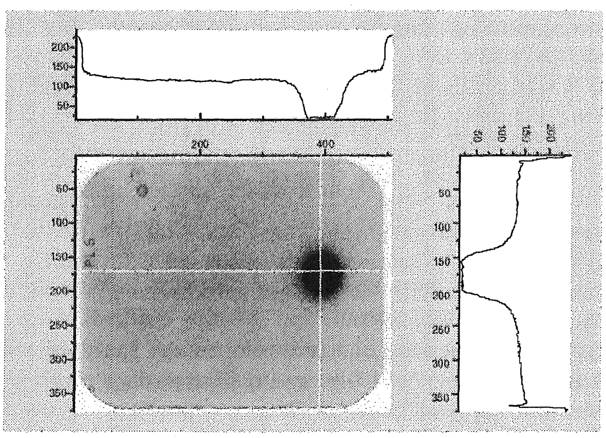

Fig. 5 The Picture of the Exposed Film and Dose Profiles

The scattering spectrums for various test materials are shown in **Figure 8**. The normalized scattering counts, S, can be expressed by the following equation.

$$S = \exp(-\mu(E)t)\frac{\mu_C}{\mu_t}p(\mu)\exp(-\mu'(E)t') \qquad (2)$$

where, μ = total attenuation coefficient of the sample material at 122 keV

μ_C = attenuation coefficient for Compton scattering of the sample material at 122 keV

$p(\mu)$ = probability that the photon scatter into the angle of μ at 122 keV

μ' = total attenuation coefficient of the sample material after collision (98 keV)

t = average thickness of the sample before collision, 1.5 cm

t' = average thickness of the sample after collision, 1.5 cm

The measured scattering counts and scattering signals calculated from Equation (2) are plotted in **Figure 9** as a function of physical density of the test materials. The measured counts are well agreed with the calculated ones. The net counts of the scattering spectrum are also summarized in **Table 2**. In the net counts calculation, the main peaks located near 98 keV, due to the 90° scattering of 122 keV photons emitting from Co-57 source, and the X-ray escape peaks located near 75 keV, due to the K X-ray accompanied with photoabsorption in the CsI detector, were considered in the calculation of detection efficiency.

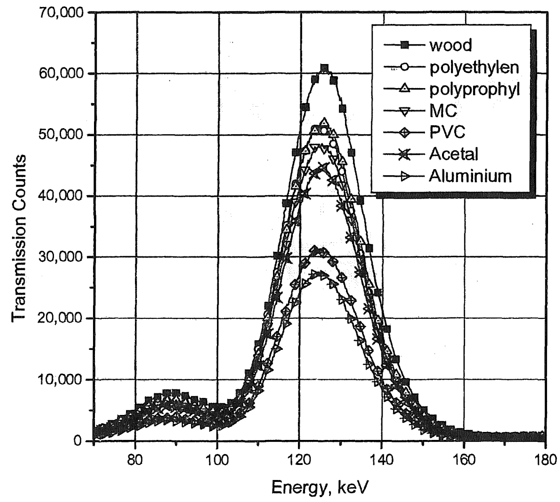

Fig. 6 Transmission Spectrum Measured by YAP

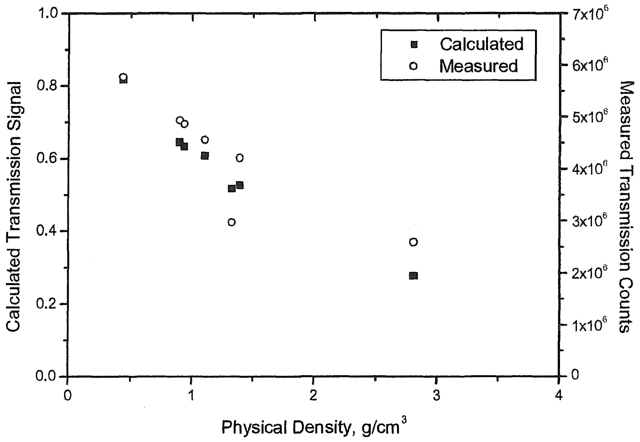

Fig. 7 Normalized Transmission Signal Calculated from Equation (1) and Measured Transmission Counts

3. Low Level and Upper Level Discrimination of Single Channel Analyzer

From the measured spectra shown in **Figures 6** and **8**, LLD and ULD were determined for the SCA inputs. For the transmission, 425 and 675 were selected for LLD and ULD values, respectively, and 200 and 500 were selected for scattering counts.

IV. Conclusions

Transmission and scattering experiments were performed to provide a basic data for developing new concept of baggage inspection system. Some materials were tested to get transmission and scattering signals. The experiment results from this work will be used in the verification of reconstruction algorithm which requires transmission and scattering signals at the same time to identify the unknown materials.

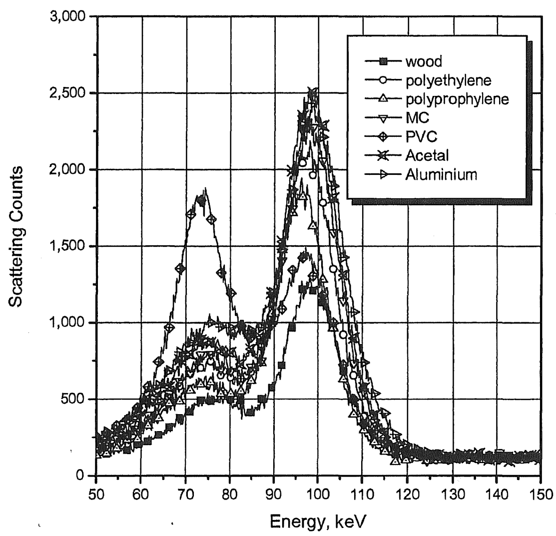

Fig. 8 Scattering Spectrum Measured by CsI

Table 2. Transmission and Scattering Net Counts for the Various Test Materials

Material	Transmission Counts	Scattering Counts
Wood	5,769,381	102,802
Polyprophylene	4,934,531	153,849
Polyethylene	4,863,505	174,182
MC	4,558,805	186,219
PVC	2,968,685	194,128
Acetal	4,208,481	209,810
Aluminum	2,594,633	219,858

Acknowledgement

This work was performed under the long-term nuclear research and development program sponsored by Ministry of Science and Technology, and sponsored by the Innovative Technology Center for Radiation Safety (iTRS).

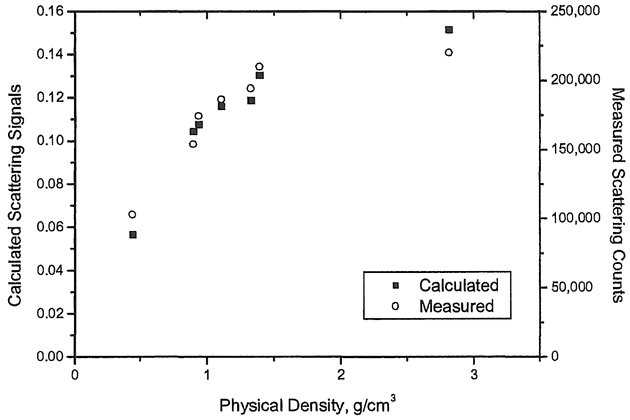

Fig. 9 Normalized Scattering Signals Calculated from Equation (2) and Measured Scattering Counts

References

1) YXLON, The use of YXLON technology in HBS Concepts at Airports, YXLON International X-Ray GmbH, 2002.
2) P.M. Bergstrom Jr., and R.H. Pratt, "An Overview of the Theories Used in Compton Scattering Calculations," *Radiat. Phys. Chem.*, 50(1), 3-29, 1997.
3) C.K. Wang, and H.K. Huang, "Calibration Procedure in dual-energy scanning using the basic function technique," *Med. Phys.*, 10(5), 628-635, 1983.
4) G. Christ, "Exact Treatment of the Dual-Energy Method in CT using Polyenergytic X-ray Spectra," *Phys. Med. Biol.*, 29(12), 1501-1510, 1984.
5) W.A. Kalender, W.H. Perman, J.R. Vetter, and E. Klotz, "Evaluation of a Prototype Dual-energy Computed Tomographic Apparatus. I. Phantom Studies," *Med. Phys.*, 13(3), 334-339, 1986.
6) R. Cesareo, F. Balogun, A. Brunetti, and C.C. Borlino, "90° Compton and Rayleigh Measurements and Imaging," *Radiat. Phys. Chem.*, 61, 339-342, 2001.
7) N.V. Arendtsz, and E.M.A. Hussein, "Energy Spectral Compton Scatter Imaging – Part I: Theoty and Mathematics," *IEEE Trans. Nucl. Sci.*, 42(6), 2155-2165, 1995.
8) N.V. Arendtsz, and E.M.A. Hussein, "Energy Spectral Compton Scatter Imaging – Part II: Experiments," *IEEE Trans. Nucl. Sci.*, 42(6), 2166-2172, 1995.
9) T.K. Tuan, *A Monte Carlo Study on a 90° Compton Scattering Imaging System by using MCNP Simulation*, Master Thesis, Hanyang University, 2003.
10) T.K. Tuan, S.H. Park, and J.K. Kim, "Development of a New Reconstruction Algorithm for Compton Scattering Imaging," Proc. ISORD-2, Sendai, Japan, July 24-25, 2003.
11) G.F. Knoll, *Radiation Detection and Measurement*, third ed., John Wiley & Sons, Inc., 2000